B(E2)↑ Measurements for Radioactive Neutron-Rich Ge Isotopes: Reaching the *N* = 50 Closed Shell

E. Padilla-Rodal,[1,2] A. Galindo-Uribarri,[1] C. Baktash,[1] J. C. Batchelder,[3] J. R. Beene,[1] R. Bijker,[2] B. A. Brown,[4,5]
O. Castaños,[2] B. Fuentes,[6] J. Gomez del Campo,[1] P. A. Hausladen,[1] Y. Larochelle,[7] A. F. Lisetskiy,[4,5] P. E. Mueller,[1]
D. C. Radford,[1] D. W. Stracener,[1] J. P. Urrego,[7] R. L. Varner,[1] and C.-H. Yu[1]

[1]*Physics Division, Oak Ridge National Laboratory, Oak Ridge, Tennessee 37831, USA*
[2]*Instituto de Ciencias Nucleares, UNAM, 04510 México, D.F., México*
[3]*UNIRIB, Oak Ridge Associated Universities, Oak Ridge National Laboratory, Oak Ridge, Tennessee 37831, USA*
[4]*National Superconducting Cyclotron Laboratory, Michigan State University, East Lansing, Michigan 48824, USA*
[5]*Department of Physics and Astronomy, Michigan State University, East Lansing, Michigan 48824, USA*
[6]*Facultad de Ciencias, UNAM, 04510 México, D.F., México*
[7]*Department of Physics and Astronomy, University of Tennessee, Knoxville, Tennessee 37996, USA*

The $B(E2; 0_1^+ \rightarrow 2_1^+)$ values for the radioactive neutron-rich germanium isotopes ^{78,80}Ge and the closed neutron shell nucleus ^{82}Ge were measured at the HRIBF using Coulomb excitation in inverse kinematics. These data allow a study of the systematic trend between the subshell closures at $N = 40$ and 50. The $B(E2)$ behavior approaching $N = 50$ is similar to the trend observed for heavier isotopic chains. A comparison of the experimental results with a shell model calculation demonstrates persistence of the $N = 50$ shell gap and a strong sensitivity of the $B(E2)$ values to the effective interaction.

The stable germanium isotopes provide a challenging testing ground for theoretical models [1]. Ge isotopes are characterized by a complex nuclear structure. The irregular dependence of the excitation energies of the first excited 0_2^+ state with the neutron number, N, and anomalies in the population cross sections for two-neutron transfer reactions [2] strongly suggest that two different configurations, based on the ground state and on the 0_2^+ state, coexist and are admixed. It is believed that the evolution of these configurations, as N increases, results in a shape transition that evolves from spherical oblate in ^{68}Ge to nearly spherical in ^{70,72}Ge to slightly prolate in ^{74}Ge and perhaps even soft triaxial in ^{76,78}Ge. Complementary studies with different probes are consistent with this interpretation [3]. A theoretical explanation about the shape coexistence phenomena has been given by the presence of intruder levels in the neutron or the proton valence shell [4]. Intruder energy states fit naturally into the neutron-proton interacting boson model plus configuration mixing [5,6]. The use of this formalism for Ge isotopes, together with a geometric interpretation, will be presented in a separate publication [7].

Extension of the studies of these interesting transitional nuclei to regions characterized by a neutron excess, including the exotic nucleus ^{82}Ge ($N = 50$), is now possible due to the availability of radioactive ion beams (RIBs). Here we report on pioneering studies of the evolution of collectivity in the neutron-rich radioactive isotopes ^{78,80,82}Ge using the reduced electric quadrupole transition probability $B(E2)\uparrow = B(E2; 0_1^+ \rightarrow 2_1^+)$ as a basic indicator of the nuclear structure. These values are usually large around midshells where the number of valence particles is maximal; likewise, low values are expected for nuclei near

the close shells, where the energy gap between 0_1^+ and 2_1^+ is larger. With only four protons outside the closed shell $Z = 28$, Ge nuclei are currently the lightest isotopic chain that allows the study of $B(E2)\uparrow$ values between the subshell closure at $N = 40$ and the major shell closure at $N = 50$.

New experimental information on nuclei far from stability constitutes a challenging test for the applicability of the shell model. For the intermediate-mass nuclei studied here ($A \sim 80$) the full pf shell with the intruder $g_{9/2}$ orbital and corresponding effective interaction are required. This is not feasible within the shell model approach nowadays; therefore, we used an effective interaction derived recently [8] for smaller configurational space which includes $p_{3/2}$, $f_{5/2}$, $p_{1/2}$, and $g_{9/2}$ orbitals with an inert ^{56}Ni core. The neutron-neutron (nn) part of the interaction was obtained from a fit to Ni isotopes with emphasis on new data between ^{66}Ni and ^{74}Ni [9]. The proton-proton (pp) part was obtained from a fit to $N = 50$ isotones, where the recently measured energy levels for ^{84}Se and ^{82}Ge were taken into account. For the proton-neutron (pn) part, the $T = 1$ component was taken to be identical to the nn part, while the $T = 0$ component was taken from the G matrix with modified monopole terms fitted to reproduce the known energies in odd-A Cu isotopes [9]. Our new $B(E2)\uparrow$ values are compared with calculations using this interaction.

The experiments described here were performed at the Holifield Radioactive Ion Beam Facility (HRIBF) at the Oak Ridge National Laboratory. The neutron-rich RIBs were produced using the isotope separator on-line (ISOL) technique that requires the use of two accelerators. A 3 g/cm^2 thick uranium carbide target was bombarded

with protons of 42 MeV energy and 7 μA average current from the $K = 100$ cyclotron. The resulting fission products are diffused out of the target material at high temperatures and transported to an ion source. After extraction from the source, the radioactive species are mass separated, converted from positive to negative ions, injected into the folded-geometry 25-MV Tandem, and delivered to the experimental area. For ISOL based RIBs isobar separation becomes one of the most important challenges. It was recognized [10] that sulfide formation provides an efficient and selective method to produce high quality beams of Ge and Sn (chemical group IV). The measurement of the RIBs of masses $A = 80$ and 82 used in the present work relied on the extraction of the molecular species $^{A}GeS^{+}$ from the production ion source. The formation of the sulfide molecule for Ge presents advantages in both purity and yield. Not only are the molecular ions SeS^{+} and AsS^{+} reduced considerably relative to GeS^{+}, but the molecular production is greater than the atomic one ($^{78}GeS^{+}/^{78}Ge^{+} = 1.4$ and $^{80}GeS^{+}/^{80}Ge^{+} = 2.5$). The ratio $^{A}GeS^{+}/^{A}Ge$ increases for shorter half-lives, implying that the release and transport of the molecular species from the production target is faster than the atomic species. This method enhances the production of isotopes farther from stability (i.e., with very short half-lives).

The data reported here come from three sets of experiments to Coulomb excite even-even isotopes of stable Se and Ge, as well as radioactive ion beams of $^{70,80,82}Ge$. In all cases (with the exception of ^{82}Ge) the beam energy was sufficiently low to ensure that the interaction between the beam and the target nuclei is purely electromagnetic and predominantly populates the first excited state. Therefore, there is no need for corrections that account for feeding from the higher-lying levels, as is the case of intermediate-energy Coulomb excitation [11]. In the first two sets of experiments, stable beams of even-even $^{70-76}Ge$, $^{74-82}Se$, and the RIBs of $A = 78$ and 80 were postaccelerated to an energy of 2.24 MeV/A and were used to bombard a 1 mg/cm^2 ^{nat}C target located at the target position of the recoil mass spectrometer (RMS). Typical beam intensities on target were 1.4×10^6 pps for $A = 78$ and 1.4×10^5 pps for $A = 80$. The determination of the $B(E2)$ values was made [12] measuring the ratios ($\sigma_{Coulomb}/\sigma_{Rutherford}$). Data were recorded as (i) single events, consisting of the recoiling target nuclei detected in the forward ring ($\theta_{mean} = 21°$) of the CsI(Tl) charged particle array HYBALL, covering the angular range $\vartheta_{c.m.} = 28°–56°$ in the center of mass, and (ii) coincidence events, with the γ rays emitted during the deexcitation of the beam nuclei detected in 8 of the twofold segmented HPGe clover detectors of the CLARION array. Since the γ rays of interest were emitted from a rapidly moving source, $v/c = 0.056$, they were subject to large Doppler broadening. The correction for this effect turned out to be of utmost importance for the $A = 78$ and 80 experiments, where the separations in energy between the $2_1^+ \rightarrow 0_1^+$ γ-ray transitions in ^{78}Ge

and ^{80}Ge and their isobaric Se contaminants are only 5 and 7 keV, respectively. Event-by-event Doppler corrections using energy and angular information from the ^{nat}C detected in HYBALL and the gammas detected in CLARION allowed an energy resolution of 3.9 keV FWHM at 614 keV and, therefore, a clear separation of the events of interest as shown in Fig. 1. These data were normalized to the adopted $B(E2)$ value of ^{74}Ge in the first experiment and to ^{80}Se in the second one. The normalization factors take into account corrections arising from efficiency, thresholds, relativistic effects, and recoil-into-vacuum deorientation.

For RIB experiments, it was necessary to monitor the beam composition in order to separate the cross section contributions from each beam component. Two different methods were used to measure the beam composition typically with less than 2% uncertainty. For the $A = 78$ experiment, projectile x-ray emission was used [13]. A beam monitoring unit consisting of a 4 mg/cm^2 ^{nat}Pd foil viewed by a LEPS HPGe detector was located after the magnetic elements of the RMS. The beam composition was determined to be 57.1% ^{78}Ge, 28.1% ^{78}Se, 9.9% ^{78}As, and 4.9% ^{78}Ga. These values are corrected for relative differences in the transmission of the isobars through the magnetic analysis section of the RMS up to the beam monitoring station. The correction factor was determined by obtaining the beam composition using a mixed beam of ^{74}Ge and ^{74}Se and by requiring that both of the adopted $B(E2)$ values [14] were reproduced correctly. This correction was not necessary for the $A = 80$ (and 82) experiments where a Bragg curve gas detector was located downstream from the target at 0° relative to the incoming beam. After purification the percentage of ^{80}Ge in the beam improved considerably from 2.2% to 95.3%.

In the third experiment, which aimed at the study of the important closed neutron shell nucleus ^{82}Ge, high γ-ray energy resolution was no longer needed. Therefore, deexcitation γ rays were detected in an array of 2×37 BaF$_2$ detectors, which provides a photopeak efficiency of 23.6%, and energy resolution of FWHM = 10% at $E_\gamma = 1$ MeV.
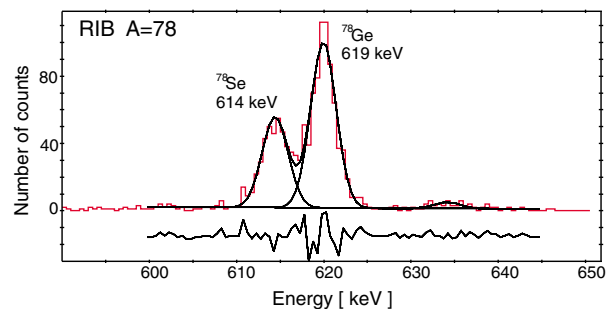

FIG. 1 (color online). Coincidence γ-ray spectrum for the $A = 78$ RIB experiment after the event-by-event Doppler correction. A clear separation between the $2_1^+ \rightarrow 0_1^+$ transitions of ^{78}Ge and ^{78}Se, differing by only 5 keV, was achieved. The fitted peaks and the resulting difference are shown at the bottom.

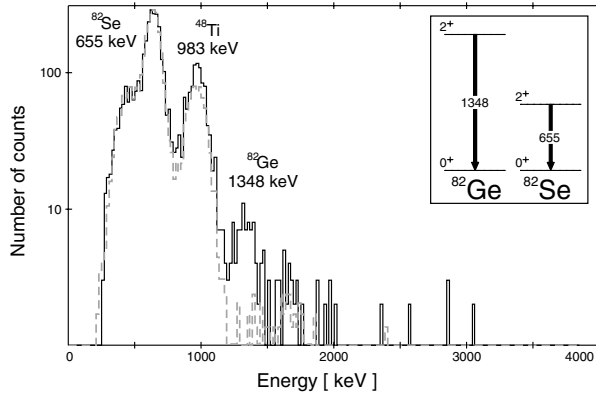FIG. 2. Overlay of the γ-ray coincidence spectra for the $A =$ 82 RIB experiment (solid line) with the one obtained with a pure ^{82}Se beam (dotted line), normalized to the Se peak.

A 300 μm Si CD type [15] microstrip detector covering $\theta_{\text{lab}} = 8°–23°$ was used to detect both the scattered beam and recoiling target nuclei. A beam energy of 220 MeV and a 99.8% enriched 1.3 mg/cm^2 ^{48}Ti target were used to increase the Coulomb excitation cross section. The $A = 82$ beam had an average intensity of 5.5×10^4 pps and a composition of 19.2% of ^{82}Ge, 1.8% of ^{82}As, and 79% of ^{82}Se after purification. The clear separation, shown in Fig. 2, between the γ-ray peaks corresponding to the beam components and ^{48}Ti allows the determination of the relative yields ^{82}Ge/^{48}Ti and ^{82}Ge/^{82}Se. A very low background under the ^{82}Ge peak was measured directly with the stable beam ^{82}Se. This was confirmed from a Monte Carlo simulation of the full γ-ray spectra using the GEANT code [16]. Above the region of interest, a very similar yield is observed for both radioactive and stable beams. These few counts arise from accidental coincidence events due to α-emitting impurities in the BaF$_2$ crystals [17]. Most of these events are suppressed by using pulse shape discrimination. The $B(E2)$ value for ^{82}Ge was determined with a relative measurement of the cross sections: $(\sigma_{\text{Coulomb}}^{\text{interest}}/\sigma_{\text{Coulomb}}^{\text{contaminant}})$ corresponding to the nucleus of interest relative to a stable isobar, present in the RIB as a contaminant, with a well known $B(E2)$ value.

All experimental $B(E2)$ values determined in this work are shown in Fig. 3. The good agreement between the measured and the adopted values [14] for the stable Ge and Se nuclei validates our experimental technique. The experimental values for the radioactive nuclei compare well with the shell model results for both the excitation energy of 2_1^+ and the $B(E2)$ (see Table I). These calculations were performed considering the complete $pf_{5/2}g_{9/2}$ model space for ^{82}Ge and ^{80}Ge, while no proton excitations to the $g_{9/2}$ orbital were allowed for ^{78}Ge. The effective quadrupole neutron (proton) charges $e_n = 0.97$ ($e_p = 1.76$) for the $E2$ transition operator were extracted from the $B(E2)$ values for ^{70}Ni (^{92}Mo). A reduction in both the excitation energy and the $B(E2)$ of 2_1^+ is expected for ^{78}Ge if a complete $pf_{5/2}g_{9/2}$-space calculation is considered.
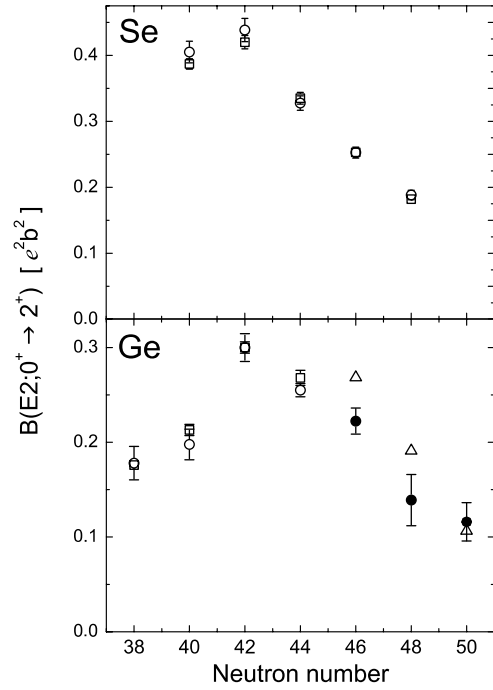

FIG. 3. Experimental $B(E2)$ values obtained in the present work (circles) for Se (top panel) and Ge (bottom panel) isotopes. A comparison with adopted $B(E2)$ values (squares) is shown for the stable nuclei. The solid circles correspond to the radioactive nuclei, which are compared with shell model calculations (triangles).

The pn-component of this effective interaction is preliminary, and changes of this part may affect the $B(E2)$ values. In the case of ^{82}Ge, only the proton degree of freedom is active and therefore no changes for the calculated $E2$ strength are expected. For ^{78,80}Ge there are neutron as well as proton contributions to the total $E2$ strength. The relative weight of these contributions depends on the strength of the pn interaction. Decreasing the interaction the weight of the proton component in the 2_1^+ state decreases, resulting in a smaller $B(E2)$. This shows that the measured $B(E2)$ values reported here represent additional important input for the reliable determination of the pn component of the effective interaction.

Figure 4 shows the $B(E2)$ values for Ni, Zn, Ge, and Se as a function of N and Z (adopted values from [14], and

TABLE I. Calculated total matrix elements $M_p = A_p e_p + A_n e_n$ for ^{78}Ge, ^{80}Ge, and ^{82}Ge isotopes. $A_n = \langle 2_1^+ \| E2 \| 0_1^+ \rangle_n$ for neutrons; $A_p = \langle 2_1^+ \| E2 \| 0_1^+ \rangle_p$ for protons. Our experimental $B(E2) \uparrow$ values and the experimental energies $E_{2_1^+}$ are compared with theoretical $B(E2; 0_1^+ \rightarrow 2_1^+) = (M_p)^2$ and $E_{2_1^+}^{\text{T}}$, respectively.

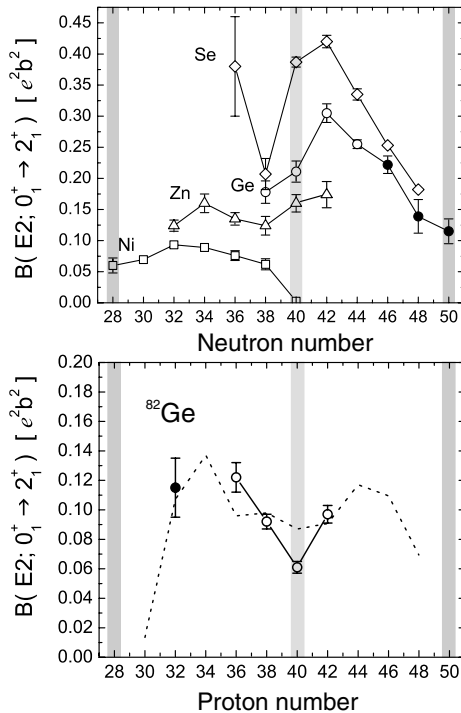|	M_p (e fm^2)	A_n (e fm^2)	A_p (e fm^2)	$B(E2) \uparrow_{\text{T}}$ (e b^2)	$B(E2) \uparrow_{\text{E}}$ (e b^2)	$E_{2_1^+}^{\text{T}}$ (keV)	$E_{2_1^+}$ (keV)
^{78}Ge	49.3	18.4	17.8	0.269	0.222(14)	642	619
^{80}Ge	43.7	13.3	17.5	0.191	0.139(27)	827	659
^{82}Ge	32.6	0.0	18.5	0.107	0.115(20)	1367	1348

FIG. 4. Trend of the experimental $B(E2)\uparrow$ values. In the top panel the behavior of the Ge chain as a function of N is compared with neighboring isotopic chains. The bottom panel shows the behavior of the $N = 50$ isotones as a function of Z compared with the shell model predictions (dotted line). Solid circles indicate RIB measurements obtained in this work.

new results from [18,19]). A clear contrast can be observed between $N = 40$ and 50. The low $B(E2)$ value recently measured for $^{68}Ni_{40}$ has been given as evidence of magicity [18]. However, the systematics for heavier nuclei do not show a drop or a strong discontinuity at this neutron number suggesting a weak effect of the $N = 40$ subshell. As we approach the $N = 50$ magic number, a smooth decrease in the $B(E2)$ values is observed. There is good agreement between the measured value of $^{82}Ge_{50}$ and the calculated value (see Table I). However, it is high compared with a simple extrapolation of the $B(E2)$ values of $^{78,80}Ge$ and the values given by systematics and various theoretical models [14]. The behavior of Ge isotopes around $N = 50$ appears to be similar to the plateau exhibited by the isotopic chains with higher-Z (not shown) such as $_{36}Kr$, $_{38}Sr$, and $_{40}Zr$. The bottom panel shows the $B(E2)$ values for the $N = 50$ isotones including ^{82}Ge which constitutes the lightest isotone reached to date. The measured value for ^{82}Ge is similar to that of ^{86}Kr and consistent with the shell model prediction which indicates that towards $Z = 28$ the $B(E2)$ value starts to decrease.

The present study of n-rich Ge isotopes using RIBs clearly illustrates that it is not always possible to apply a "universal" experimental technique to the measurement of a physical property along an isotopic chain. The small

energy separation between the $2^+_1 \rightarrow 0^+_1$ γ-ray transitions of $^{78,80}Ge$ and their corresponding isobaric beam contaminants $^{78,80}Se$ represented a challenge, which was further complicated by the decrease in the beam intensity, purity, and cross section as we move away from stability. The new information on the $E2$ transition strengths constitutes a stringent test for the nuclear models, as was illustrated for the pn-part of the shell model effective interaction. The experimental trend found around $N = 50$ for the Ge isotopes is well reproduced within the framework of the shell model. This suggests that $N = 50$ indeed persists as a good magic number for Ge.

[1] See, e.g., relevant references in *Nuclear Structure of the Zirconium Region*, edited by J. Eberth, R. A. Meyer, and K. Sistemich (Springer-Verlag, Berlin, 1988).

[2] R. Lecomte *et al.*, Phys. Rev. C **25**, 2812 (1982), and references therein.

[3] H. T. Fortune and M. Carchidi, Phys. Rev. C **36**, 2584 (1987).

[4] K. Heyde *et al.*, Nucl. Phys. **A466**, 189 (1987).

[5] P. Duval and B. Barrett, Nucl. Phys. **A376**, 213 (1982).

[6] P. Duval, D. Goutte, and M. Vergnes, Phys. Lett. **124B**, 297 (1983).

[7] E. Padilla-Rodal, Ph.D. thesis, Universidad Nacional Autónoma de México, 2004 (to be published).

[8] A. F. Lisetskiy, B. A. Brown, M. Horoi, and H. Grawe, Phys. Rev. C **70**, 044314 (2004).

[9] A. F. Lisetskiy, B. A. Brown, and M. Horoi, in Proceedings of the ENAM04 Conference (to be published), and references therein.

[10] D. W. Stracener *et al.*, Nucl. Instrum. Methods Phys. Res., Sect. A **521**, 126 (2004).

[11] B. V. Pritychenko *et al.*, Phys. Lett. B **461**, 322 (1999); T. Motobayashi *et al.*, Phys. Lett. B **346**, 9 (1995); H. Iwasaki *et al.*, Phys. Lett. B **522**, 227 (2001); V. Chisté *et al.*, Phys. Lett. B **514**, 233 (2001).

[12] D. C. Radford *et al.*, Phys. Rev. Lett. **88**, 222501 (2002).

[13] J. E. McAninch *et al.*, Nucl. Instrum. Methods Phys. Res., Sect. B **99**, 541 (1995).

[14] S. Raman *et al.*, At. Data Nucl. Data Tables **78**, 1 (2001).

[15] S2 detector, Micron Semiconductor Limited, Sussex, U.K.

[16] Geant Detector Simulation Tool, CERN, 1993, http://wwwinfo.cern.ch/asd/geant.

[17] F. A. Beck, in *Proceedings of the International Conference on Instrumentation for Heavy Ion Nuclear Research*, edited by D. Shapira (Harwood Academic Publishers, Amsterdam, 1985), p. 129.

[18] O. Sorlin *et al.*, Phys. Rev. Lett. **88**, 092501 (2002).

[19] S. Leenhardt *et al.*, Eur. Phys. J. A **14**, 1 (2002).